Investigation of physico-chemical behaviour of local anaesthetics in aqueous SDS solutions†

Emilia Iglesias

Received (in Montpellier, France) 31st October 2007, Accepted 11th December 2007
First published as an Advance Article on the web 10th January 2008
DOI: 10.1039/b716813f

The behaviour of local anaesthetics tetracaine (TCA), procainamide (PAM) and novocaine (NOV) in aqueous sodium dodecyl sulfate (SDS) solutions has been investigated by steady-state fluorescence emission spectroscopy, electrical conductance and reaction kinetics. A sharp increase of fluorescence emission of local anaesthetics (LA) in aqueous surfactant solutions at concentrations close to the critical micelle concentration (cmc) was observed due to the formation of premicellar aggregates. Plots of the specific conductance, κ, against [SDS], measured in the presence of a fixed amount of LA, clearly had two break points. Rates of the alkaline hydrolysis of the ester function of LA were dramatically reduced in the presence of SDS at concentrations close to the cmc ($\sim$8.3 mM). Both the increase in fluorescence emission intensity and the reduction of hydrolysis reaction rates occur within a very narrow range of SDS concentration near the cmc and then level off/down. The strongest incorporation into negatively charged micellar aggregates was observed for TCA, the anaesthetic having the strongest hydrophobicity, and the weakest incorporation was observed for PAM, the least hydrophobic molecule. This result is important in the correlation of the anaesthetic potency of LA with their hydrophobicity.

Introduction

The interface at the polar head groups of micelles in the presence of surrounding aqueous medium provides distinct microenvironments in different concentration ranges, wherein changes in both physical and chemical properties of a probe usually occur, and represent models by which one might study the chemical behaviour of membrane systems. Above the critical micelle concentration (cmc), ionic surfactants in water form aggregates of various sizes, shapes, and dispersity. A variety of simple techniques, wherein an appropriate property is monitored as a function of concentration, can be used in cmc determination.[1–3] Premicellar aggregation behaviour is one of the most interesting subjects for understanding the self-assembly of surfactants in aqueous solutions. Some surface-active agents form premicellar aggregates at a concentration below the cmc. This is a rather general effect observed in geminine surfactant solutions with assumed aggregation number as low as 2–5[4,5] but is not exclusive to these surface active agents, which usually contain two alkyl chains joined together by spacers; in fact, other systems show premicellar aggregation effects.[6–8] Recently, Ramakrishnan *et al.*[9] demonstrated that several surfactants that contain a NLO (non-linear optical) chromophore, either at the hydrocarbon tail, or at the hydrophilic head group, or even as a counterion, form small premicellar aggregates at surfactant concentrations as small as 0.6 mM for an alkyl chain of 12 C-atoms (the usual value for the free surfactant in water is 14 times higher).[10] During the past few years, biophysical study of biological macromolecules has become an important area of research because of their ability to achieve specific chemical efficiency because of organization in the reaction media. In this sense, most of the local anaesthetics now in use are amphiphilic molecules containing both a hydrophilic group (usually an amine moiety) and a hydrophobic group that generally contains an aromatic ring.[11–13]

In this article, we report the analysis of the interactions in water of the anionic surfactant SDS and the LA whose structures are shown in Scheme 1, by using fluorescence measurements, electrical conductance, and the kinetic study of the hydrolysis of the ester function. The hydrophilic group of these LA is a tertiary amine (with ethyl- or methyl-substituents) that is protonated at approximately pH $<$ 10. The hydrophobic group is a *p*-aminobenzamide or a *p*-aminobenzoate, which are prototypes of NLO chromophores. The presence of these drugs provokes micellization that accompanies strong changes in both fluorescence emission and rates of hydrolysis. Electrical conductance of aqueous binary mixtures of SDS and these LA points to the formation of small premicellar aggregates at surfactant concentrations below the cmc (8.3 mM in water).[10,14,15]

Experimental

The LA were purchased from Sigma with purity higher than 99% in the form of the hydrochloride salts of their ammonium ions and were used as received. The other reagents were

Departamento de Química Física e E. Q. I, Facultad de Ciencias, Universidad de La Coruña, 15071-La Coruña, Spain. E-mail: qfemilia@udc.es

† Electronic supplementary information (ESI) available: Figs. S1–S4 showing, respectively, the spectrophotometric titration of TCA; the linear increase of electrical conductance with the LA concentration; the linear increase of observed rate constants, k_o, in hydrolysis with [OH^-], and the influence of SDS concentration on rates of hydrolysis at [OH^-] = 0.40 M for TCA. See DOI: 10.1039/b716813f

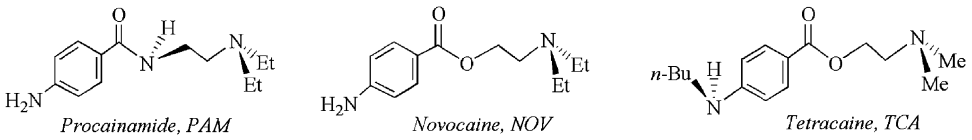

Scheme 1 Molecular structures of local anaesthetics, LA.

commercially available products of the maximum purity and were used without further purification. Solutions were freshly prepared with double distilled water over potassium permanganate.

The pH was controlled using buffer solutions of acetic acid–acetate and their chloro-derivatives and was measured with a Crison 2001 pH-meter equipped with a GK2401B combined glass electrode and calibrated using commercial buffers of pH 4.01, 7.02, and 9.26 (Crison). The reported [buffer] refers to the total buffer concentration.

The UV–Vis spectra and kinetic experiments were recorded with a Kontron-Uvikon double beam spectrophotometer fitted with thermostatted cell holders and following the decrease in absorbance at wavelengths around 300 nm. Data acquisition of both UV–Vis spectra and kinetics was performed with software supported by the manufacturer and converted to ASCII format for their analysis with common program packages. The kinetic measurements of absorbance (A) *versus* time (t) always fitted the first-order integrated rate-equation quite satisfactorily ($r > 0.999$). Experimental data were fitted to the equation $A = A_\infty + (A_o - A_\infty)\exp(-k_o t)$ by non-linear regression analysis, to obtain k_o, A_∞, and $(A_o - A_\infty)$ as optimizable parameters (with A, A_o, and A_∞ being the absorbance readings at times t, zero and infinity, respectively; k_o represents the pseudo-first order rate constant, and $\exp(x) = e^x$). Commercial software packages such as Fig. P-60 or Origin were used to perform the regression analysis, as well as to edit figures. The standard deviations that affect the optimizable parameters reported in the Tables correspond to those obtained in the fitting process.

Steady-state fluorescence spectra were recorded on an Aminco-Bowman Series 2 spectrofluorometer at 25 °C. Excitation and emission slits were fixed at 4 and 2 nm, respectively, the excitation wavelength was set near 300 nm (depending on the drug), and the emission intensity of fluorescence was recorded at around 350 nm. In all measurements the emission spectrum, collected from 315 to 430 nm, was obtained from solutions of constant drug concentration and variable SDS concentration (or organic solvent percentage). The drug concentration was chosen in such a way that the absorbance of the sample at the excitation wavelength was lower than 0.2 absorbance units.

Specific conductivities were measured in a Knick conductimeter provided with a four-pole measuring cell (the measured cell-factor was equal to 1.10 cm^{-1}) and temperature sensor, using solutions prepared with doubly distilled water and following the extraction–dilution method[14] by using a two-syringe automatic titrator, Crison 2S, programmed for V_{in}/V_{out} equal to 5 mL/5 mL. The solutions were thermostatted in a jacketed beaker, equipped with a magnetic stirring device, and the temperature was held constant within ±0.01 °C. The conductivity of the aqueous solutions was measured as a function of the drug concentration for the binary drug/water system, and as a function of SDS concentration, keeping constant the concentration of the drug for the ternary SDS/drug/water system.

Results

Absorption spectra

The UV–Vis spectrum of diluted (~60 μM) aqueous solutions of compounds, depicted in Scheme 1, shows two broad bands near 220 nm ($S_o \rightarrow S_2$) and 300 nm ($S_o \rightarrow S_1$) due to (π, π^*) and (n, π^*) transitions, respectively. The position of the maximum wavelength absorption, λ_{max}, depends on the molecular structure of the sample, but the absorption intensity is mainly determined by the experimental conditions. Fig. 1a

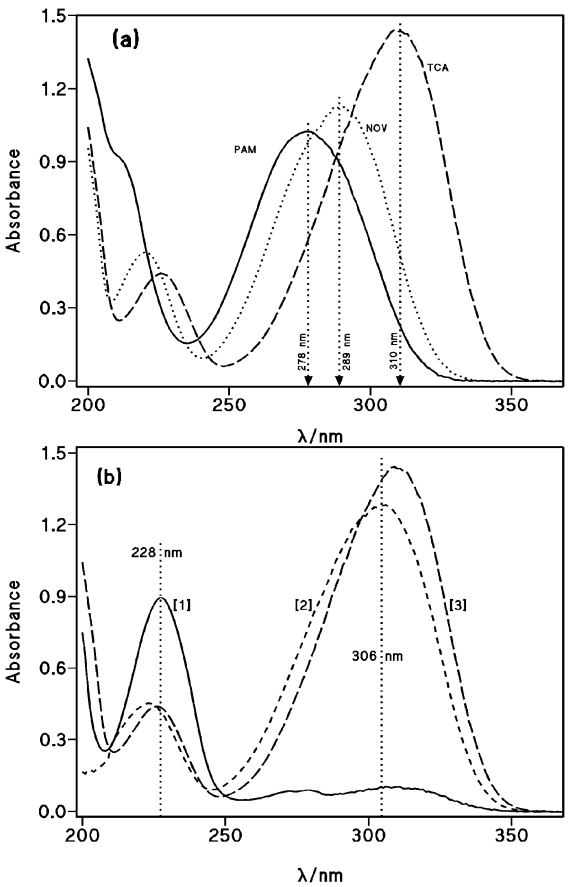

Fig. 1 (a) Absorption spectra of PAM (62 μM), NOV (63 μM), and TCA (61 μM) in aqueous buffered solutions of acetic acid–acetate (3 mM) of pH 4.75; and (b) absorption spectra of aqueous solutions of TCA (6.1×10^{-5} M) in [1] strong acid medium at $[H^+] = 0.037$ M (HCl); [2] alkaline medium of $[OH^-] = 0.037$ M; and [3] aqueous acetic acid–acetate buffer 3 mM of pH 4.75.

Table 1 Spectral characteristics of PAM, NOV, and TCA observed in aqueous solutions of the drug (~60 μM) under different acid–base conditions (strong acid, mild acid, and alkaline media), and values of acidity constants of the primary (or secondary) amine group, pK_{a1}, measured in this work at 0.30 M of total buffer concentration, and of the tertiary amine group, pK_{a2}, collected from the literature.[13,16,17] Values of ΔpK_{a2} refer to the difference between the excited and ground states of the tertiary amine group

Drug (CAS number)	λ (SH_2^{2+})/nm	λ (SH^+)/nm	λ (S)/nm	pK_{a1} (SH_2^{2+})	pK_{a2} (SH^+)	ΔpK_{a2} (SH^+)
PAM (51-06-09)	223	278	278	2.72 ± 0.05[a]	9.86 ± 0.25	1.67
NOV (59-46-21)	227	220/289	215/280	2.31 ± 0.05[b]	9.24 ± 0.25	2.80
TCA (94-24-6)	228	226/310	223/306	2.27 ± 0.02[a]	8.24 ± 0.28	0.67

[a] Determined in this work. [b] Ref. 18.

shows the spectra of TCA, NOV and PAM in mild acid medium, whereas the spectrum of TCA recorded under different experimental conditions is shown in Fig. 1b.

A small shift in λ_{max} to shorter wavelengths was observed on going from mild acid—or neutral—medium to alkaline medium, due to deprotonation of the tertiary amine group. Tertiary amines are strong bases in water, in such a way that the addition of the hydrochloride salts to water yields the corresponding alkylammonium ions. Values of the highest pK_a (denoted by pK_{a2}) corresponding to the protonated tertiary amine group (symbolized by SH^+) were collected from the literature[13,16,17] and are listed in Table 1, along with the spectral characteristics of these drugs under different conditions. By contrast, in strong acid medium, the absorption band around 300 nm almost disappears, due to the protonation of the primary (or secondary) amine group. The decrease of absorbance with pH was followed to measure the pK_{a1} of this group. The pK_a of primary arylamines ranges from 5 to less than zero, depending on the nature of the substituent and on its position in the ring.[16,17] Aromatic secondary amines have similar base strength. Arylamines that contain strongly electron-withdrawing groups are weak bases and their pK_a can be determined by spectrophotometric titration. This method has been followed in this study to measure the first pK_{a1} as a result of the fit of the experimental data, *A*–pH, to eqn (1). The *A versus* pH curve shows a sigmoidal shape and has an inflection point at pK_{a1}. As an example, in the case of TCA the input values of $A_a = 0.025$—the absorbance reading at the lowest pH—and $A_b = 0.924$—the absorbance reading at the highest pH—gave the optimized $pK_{a1} = 2.27 \pm 0.02$ reported in Table 1, along with the pK_{a1} measured for the other anaesthetics.[18] (See Fig. S1 of ESI†.)

$$A_{312} = \frac{A_a 10^{pK_{a1}} + A_b 10^{pH}}{10^{pK_{a1}} + 10^{pH}} \qquad (1)$$

Amides (the linked group in procainamide) are not basic enough for their pK_a values to be accurately measured in water. Then, under the experimental conditions of this work, the amide group of procainamide is a neutral group.[16]

Fluorescence measurements

Profound changes in the acidity or basicity of an organic molecule often accompany the absorption of a quantum of visible or UV-light. An estimation of the variation in pK_a (ΔpK_a) of an electronic excited species can be made from the changes observed in its UV–Vis absorption spectra observed on protonation or deprotonation. Following the treatment of Förster,[19] at 25 °C the formula that relates ΔpK_a (= $pK_a^* - pK_a$) to the shift in wavelength absorption is given by eqn (2), where ΔpK_a is the difference in the pK_a of a given acidic species (*e.g.* SH^+) in the excited and ground state, and λ_1 is the maximum wavelength absorption of S (the conjugate base) and λ_2, that of SH^+.

$$\Delta pK_a \approx 2.1 \times 10^4 \left(\frac{1}{\lambda_1(\text{nm})} - \frac{1}{\lambda_2(\text{nm})} \right) \qquad (2)$$

The results collected in Table 1 indicate that the UV–Vis absorption spectra of PAM, TCA and NOV show a blue shift (hypsochromic shift) on increasing pH, see Fig. 1b for the case of TCA. Then, we can calculate a positive change in pK_{a2} (the acid SH^+ becomes weaker) of approximately 1.7, 0.7 and 2.8 units, respectively for PAM, TCA and NOV. The same trend was observed for the diprotonated species, however the effect is smaller. These spectroscopic observations ensure that in aqueous acetic acid–acetate buffer the LA studied here maintain a protonated tertiary N-amine even in the excited state, and under alkaline media of pH > 12 both amine-N are unprotonated.

Therefore, we used fluorescence measurements to evaluate the binding constants of the LA to SDS micelles under experimental conditions of cationic drug (protonated tertiary amine-N, SH^+) obtained in aqueous solutions of acetic acid–acetate buffer, and of neutral drug (S), obtained in aqueous alkaline media. The characteristic of these organic molecules of possessing electron donor and acceptor groups linked by a single bond leads to enhanced fluorescence in media of reduced polarity, because the excited states of these molecules decay by rotation of the aniline group around the N–phenyl bond toward an emissive 'twisted intramolecular charge transfer state'.[20,21] Consequently, when these molecules are trapped in micellar aggregates, they exhibit enhanced fluorescence with emission maxima shifted to shorter wavelength (with respect to that in the bulk water environment) due to the increase in radiative rate, the decrease in rotational freedom, and the elimination of quencher water molecules from the immediate surroundings.

The effect of decreasing the amount of water molecules can be seen in Fig. 2a which shows the non-linear rise of fluorescence emission intensities from excited PAM, TCA and NOV as the methanol percentage increases. Fig. 2b shows the effect of both the elimination of quencher water molecules and the reduction of rotational freedom of fluorophores as a consequence of being trapped inside the SDS micelles. In Fig. 3a and 3b we try to offer a comparison between different experimental conditions in the fluorescence emission of the same drug, PAM and TCA, respectively.

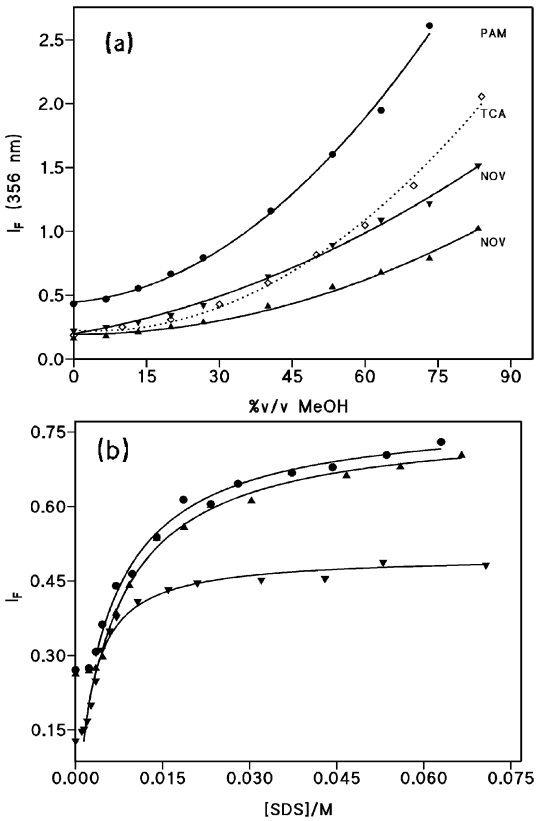

Fig. 2 Fluorescence intensities of (a) (●) PAM 8.3 μM, (◇) TCA 3.3 μM, and of NOV 16.7 μM at (▼) $[OH^-] = 0.016$ M, and (▲) neutral, measured as a function of MeOH percentage; and (b) (▼) NOV (14.7 μM) measured at 346 nm in aqueous alkaline ($[OH^-] = 0.037$ M) solutions and of PAM (11 μM) measured at 355 nm in aqueous alkaline (▲) $[OH^-] = 0.015$ M and (●) $[OH^-] = 0.037$ M solutions, as a function of [SDS].

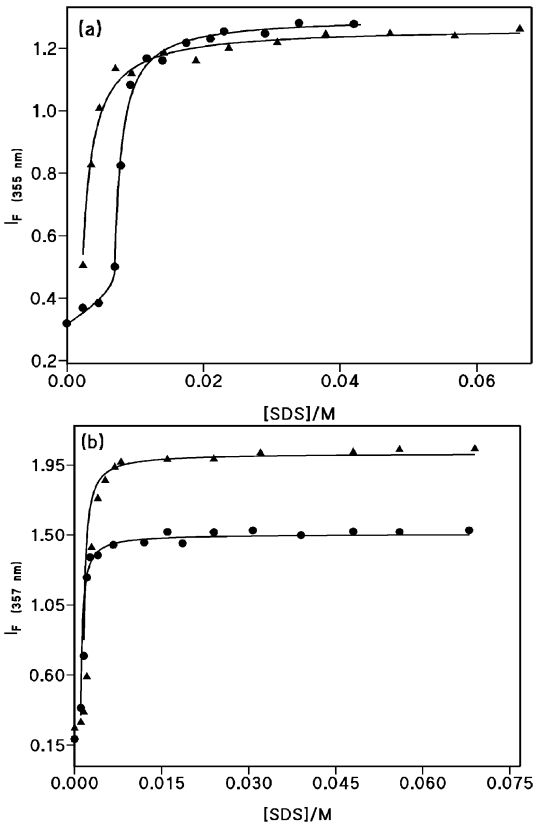

Fig. 3 Fluorescence intensities of (a) PAM (11 μM) in neutral (●) and (▲) buffer of acetic acid–acetate 0.1 M pH 4.73 as a function of [SDS]; and of (b) TCA (5.4 μM) measured in (●) acetic acid–acetate buffer 0.10 M of pH 4.73 and in (▲) alkaline medium, $[OH^-] = 0.037$ M as a function of [SDS]. Curves fit eqn (3).

Results in methanol–water solutions reflect the specific solvent interactions with the fluorophore, whereas results in aqueous SDS surfactant solutions indicate association of fluorophores (LA) to micellar aggregates at the onset of micellization, either when the LA is a cationic (SH^+) or a neutral species (S). The abrupt increase of fluorescence intensity observed even at [SDS] below the cmc, reveals a strong association of the LA to SDS micelles by provoking micellization. In addition, the fact that the I_F values obtained at high [SDS]—mainly for NOV and PAM—were much lower than those observed at high MeOH percentages suggests that the fluorophore is located inside the micelles in a very hydrated region.

Taking into account that fluorophores have different lifetimes in water and in solvents (the microenvironment of the probe in the micelles resembles organic solvents), Scheme 2 can be proposed to quantitatively explain the results. Measurements of fluorescence intensities in water (I_F^w), at 100% incorporation to the micelles (I_F^m), and at intermediate micelle concentration (I_F), allow determination of the binding constant, K_s. By considering the proportionality of fluorescence intensity to fluorophore concentration, *i.e.* $I_F = I_F^w + I_F^m$, and that $[S_t] = [S_w] + [S_m]$, the eqn (3) can be derived. This equation can be applied when the emission quantum yield is independent of surfactant concentration; in other words, the counterions do not quench the probe, as is observed experimentally since no decrease in fluorescence intensity was noted at high surfactant concentration.

$$I_F = \frac{I_F^w + I_F^m K_s [SDS]_m}{1 + K_s [SDS]_m} \qquad (3)$$

The experimental results were quantitatively analysed by eqn (3), with the experimental input values and the optimized results depicted in Table 2. A special mention of the data obtained with TCA is needed in order to remark that, because of the abrupt increase of I_F within a very narrow [SDS] interval, the convergence of the fitting process is not easy.

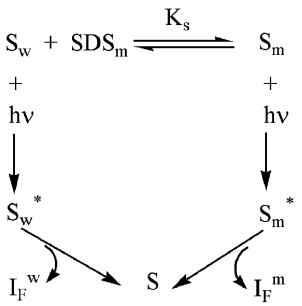

Scheme 2 Proposed steps of fluorescence emission in micellar solutions.

Table 2 Values of binding constants of PAM, NOV, and TCA to SDS micelles, K_s, and cmc determined at low surfactant concentrations from steady-state fluorescence measurements

Anaesthetic	Medium	I_F^w	I_F^m	K_s/mol^{-1} dm^3	cmc/10^{-3} M
PAM (11 μM)	[OH$^-$] = 0.037 M	0.271	0.79 ± 0.02	115 ± 10	1.1
	[OH$^-$] = 0.015 M	0.261	0.77 ± 0.01	97 ± 8	1.2
NOV (14.7 μM)	[OH$^-$] = 0.037 M	0.128	0.489 ± 0.007	445 ± 28	1.0
TCA (5.4 μM)		0.225	2.05	3350 ± 270	1.2
PAM (11 μM)	Buffer, 0.1 M, pH 4.73	0.32	1.266 ± 0.015	816 ± 69	2.0
TCA (5.4 μM)		0.190	1.505	3750 ± 315	1.0

To solve this inconvenient problem, only the K_s parameter was optimized, however the starting input values were those obtained in the kinetic experiments, *vide infra*. The curves shown in Fig. 3b have been drawn with the results listed in Table 2.

Electrical conductance

The electrical conductance of aqueous solutions of SDS surfactant containing a fixed amount of the LA was measured so as to observe premicellar aggregates.

Drug solutions were prepared by dissolving the desired amount of the hydrochloride salt ($<10^{-2}$ M) in the appropriate volume of water. The specific conductance, κ, of these solutions increases proportional to the salt concentration for the investigated temperature interval 15–25 °C, see Fig. S2.† The conductance is due to both the alkylammonium cation (λ_{SH^+}) of the LA and the chloride anion (λ_{Cl^-}) and plots of κ *versus* [LA]$_t$ were perfect straight lines, whose slope equals the molar conductivities of contributing ions, $\sum\lambda_i$ ($= \lambda_{SH^+} + \lambda_{Cl^-}$) reported in Table 3 (second row).

The variation of κ with the SDS surfactant concentration measured for the ternary SDS/LA/water system at fixed LA concentration is shown in Figs. 4 and 5 for the cases of NOV and TCA, respectively. Two break points can clearly be seen: one is observed at SDS concentration slightly higher than the cmc of pure SDS aqueous solutions (Table 3, row 6) and the other appears at SDS concentration 4-fold lower than the cmc. In between these two break points, we have observed the greatest variation for fluorescence measurements, *vide supra*, and for rates of hydrolysis reaction, *vide infra*. The slope value ($\sim 26\ \Omega^{-1}$ cm^2 s^{-1}, represented in general by B_1) of the straight line of the up-part of the curve is quite similar to that determined for pure SDS (25.8 Ω^{-1} cm^2 s^{-1}).

In accordance with the work of Bales *et al.*,[22] we assumed an aggregation number of $N_{agg} = 50$ for SDS micelles at low surfactant concentration (close to the cmc) and in the absence of salts. Then the concentration of micelles is of the same order as that of LA molecules, which means that the number of LA molecules per micelle is small so as to expect important changes in the nature of SDS micelles. Nevertheless, the effect produced in the micelle ionization degree, α, determined as the ratio of B_1/B_2, with B_2 being the slope of the straight line portion in between the two break points, is significant: it increases from 0.35 for pure SDS to 0.50 in the presence of 0.7 mM of novocaine. Also worthy of comment is the different behaviour observed below the lowest break point in the case of TCA with respect to NOV, and the low value calculated for B_3 ($= 36\ \Omega^{-1}$ cm^2 s^{-1}) with TCA, which is much lower than the sum of the molar conductivities of the contributing ions, dodecyl sulfate (λ_{SD^-}) and sodium (λ_{Na^+}). This fact suggests aggregation between TCA and SDS monomers with an important degree of neutralization, the phenomenon of which leads to the nonsense value of $\alpha = 1.68$ ($= B_2/B_3$) obtained if we consider that below the lowest break point there are no micellar aggregates.

Hydrolysis reaction

The ester function of TCA and NOV molecules hydrolyses at slow rates in aqueous alkaline medium. The kinetic study of the reaction has been conducted by conventional UV–Vis spectroscopy noting the decrease in absorbance at 320 nm ($\Delta\varepsilon \approx 18\,000$ mol^{-1} dm^3 cm^{-1}) and 285 nm ($\Delta\varepsilon \approx 8600$ mol^{-1} dm^3 cm^{-1}), respectively for TCA and NOV.

Table 3 Molar ionic conductivities ($\sum\lambda_i$) of ions SD$^-$ and Na$^+$, in the case of SDS aqueous solutions, and of SH$^+$ (representing the NOV or TCA molecule protonated on the tertiary amine-N) and Cl$^-$, determined from the slope of the plots of κ *versus* [SDS]—below the cmc—or *versus* [NOV] or [TCA], and intercepts (A_i) and slopes (B_i) of the linear plots observed in the variation of specific conductance, κ, with [SDS] at a constant [NOV] or [TCA]

Parameter	SDS	NOV	TCA
$\sum\lambda_i/\Omega^{-1}$ cm^2 mol^{-1}	65.8 ± 0.5 (25 °C)	101.35 ± 0.08 (25 °C)	90.8 ± 0.3 (25 °C)
($\lambda_{SD^-} + \lambda_{Na^+}$ or $\lambda_{SH^+} + \lambda_{Cl^-}$)		83.8 ± 0.2 (15 °C)	72.3 ± 0.2 (15 °C)
Parameter	SDS	SDS + NOV (0.775 mM)	SDS + TCA (0.83 mM)
A_1/mS cm^{-1}	0.338 ±0.004	0.370 ± 0.007	0.363 ± 0.008
B_1/Ω^{-1} cm^2 mol^{-1}	25.78 ± 0.15	26.4 ± 0.2	26.6 ± 0.2
cmc/mM	8.3	9.8	9.0
α (Ionization degree)	0.35	0.50	0.44
A_2/mS cm^{-1}	(7 ± 2)	0.113 ± 0.004	0.061 ± 0.0015
B_2/Ω^{-1} cm^2 mol^{-1}	65.8 ± 0.5	52.7 ± 0.6	60.2 ± 0.4
cmc/mM	—	2.3	0.87
α (Ionization degree)		0.77	1.68
A_3/mS cm^{-1}	—	(7.76 ± 0.01) × 10^{-3}	0.082 ± 0.004
B_3/Ω^{-1} cm^2 mol^{-1}	—	68.1 ± 0.2	35.9 ± 0.8

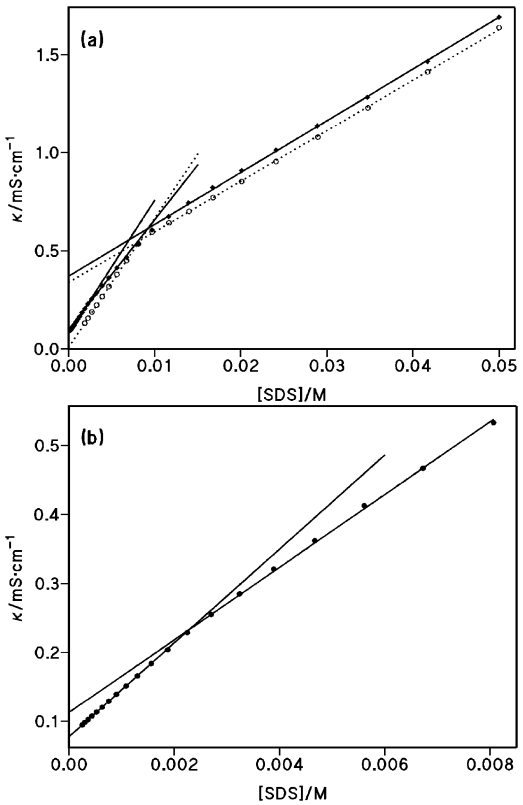

Fig. 4 (a) Plots of the specific conductance, κ, of aqueous solutions of (○) SDS and (●) SDS + [NOV] = 0.775 mM as a function of SDS concentration at 25 °C; (b) expanded plot of SDS + NOV (0.775 mM) aqueous solution below the first break point.

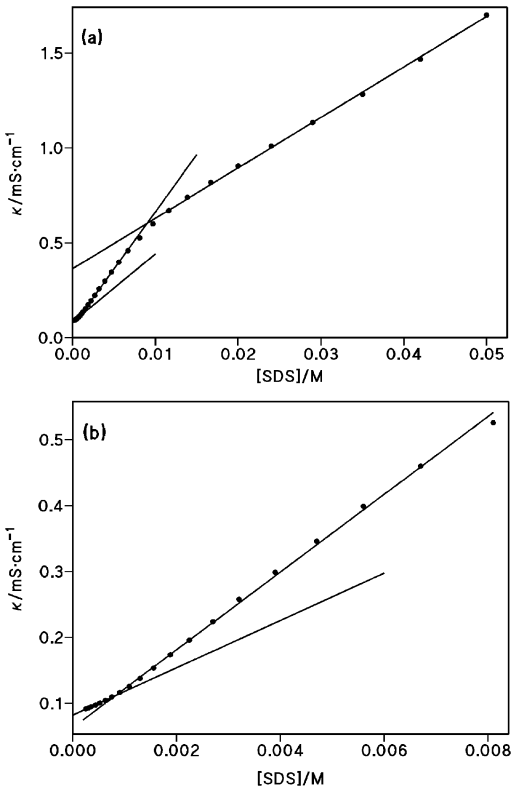

Fig. 5 (a)Specific conductance of aqueous solutions of SDS measured at 25 °C in the presence of [TCA] = 0.83 mM; (b) expanded plot below the first break point.

Under pseudo-first order conditions with the local anaesthetic as the limiting reagent ([LA] $\approx 6 \times 10^{-5}$ M and [OH^-] > 0.1 M), the integration method has been applied to record the absorbance–time (A–t) data, during at least 2.5 half-lives, and fit the data to the first-order integrated rate equation (see the Experimental section). In every experiment, perfectly first-order behaviour was observed.

Values of k_w (k_o in water) increase proportional to [OH^-], the hydrolysis by the solvent being negligible (Fig. S3†), then eqn (4) applies, with $k_{OH} = (2.87 \pm 0.03) \times 10^{-3}$ mol^{-1} dm^3 s^{-1} for the case of TCA at 25 °C and $k_{OH} = (4.23 \pm 0.05) \times 10^{-3}$ mol^{-1} dm^3 s^{-1} for the hydrolysis of NOV at the same temperature.[23]

$$k_w = k_{OH}[OH^-] \quad (4)$$

Subsequently, we analyzed the effect of SDS concentration on the ester hydrolysis of both TCA and NOV. In both cases, the addition of SDS produces a dramatic decrease of the hydrolysis rate at [SDS] < 8.3 mM (the cmc of pure SDS solutions). Figs. 6 and 7 show the variation of k_o as a function of SDS concentration.

It is important to note the enormous inhibition effect, higher than 100 times, and the narrow surfactant concentration interval required to observe the maximum reduction effect. These facts indicate a strong interaction of LA molecules (which are neutral substrates under the reaction conditions) with SDS monomers to provoke the appearance of premicellar aggregates. These negatively charged premicellar aggregates entrap the LA molecules, wherein they are protected from the attack of the OH^- nucleophile, because of the equal-charge repulsions with the micelle surface. Scheme 3 accounts for the experimental observations, from which eqn (5) can be deduced, where the micellized surfactant concentration, $[SDS]_m = [SDS]_t - cmc$, have been determined from the cmc values reported in Table 4, which were determined as the input values

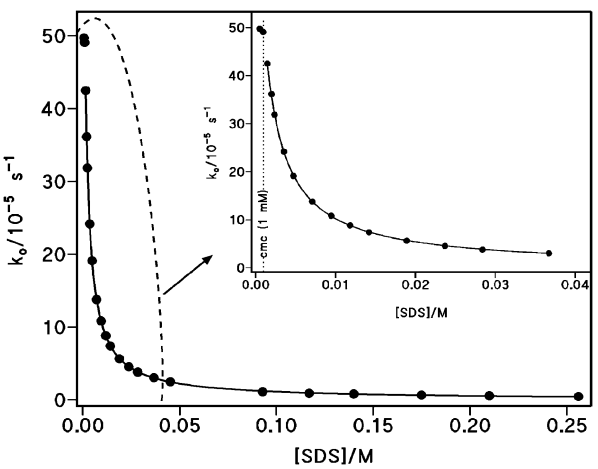

Fig. 6 Influence of SDS concentration on the alkaline hydrolysis of novocaine at [OH^-] = 0.13 M, [NOV] = 58 μM, and 25 °C. Inserted figure shows points close to the cmc (~1.0×10^{-3} M). Curves fit eqn (5).

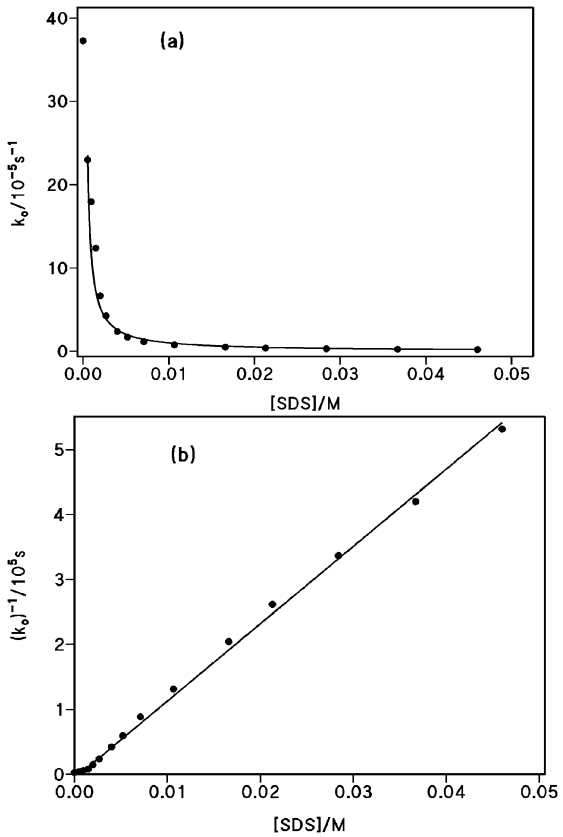

Fig. 7 (a) Influence of SDS on the alkaline hydrolysis ([OH^-] = 0.13 M) of TCA (57 μM) at 25 °C; (b) reciprocal plot of k_o against [SDS] according to eqn (5).

that give the best fit of eqn (5) to the experimental data.

$$k_o = \frac{k_{OH}[OH]_w}{1 + K_S[SDS]_m} \quad (5)$$

Curves in Figs. 6 and 7, and S4† correspond to the fit of eqn (5) to the experimental data when the optimized parameters: K_s, the binding constant of LA to the premicellar aggregates; cmc, the kinetic critical micelle concentration, and k_w (= $k_{OH}[OH^-]$ are those reported in Table 4. The reciprocal plot of k_o *versus* [SDS] is displayed in Fig. 7b; a good straight line is observed in accordance with eqn (5).

Discussion

Water (μ = 1.82 D, ϵ = 78.3) and MeOH (μ = 1.71 D, ϵ = 32.66) are hydrogen bond donor solvents with similar dipole moments but different dielectric constants. The enhanced fluorescence in water–methanol mixtures may be due to the

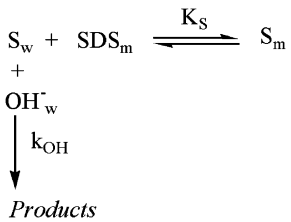

Scheme 3 Reaction scheme for hydrolysis.

Table 4 Values of binding constants and cmc obtained in the study of the influence of SDS on the alkaline hydrolysis of TCA and NOV at 25 °C

[Drug]/μM		[OH^-]/M	$k_w/10^{-4}$ s^{-1}	K_s/mol^{-1} dm^3	cmc/M
TCA	57	0.13	3.73 ± 0.08	3460 ± 370	0.4×10^{-3}
		0.40	11.6 ± 0.2	4500 ± 250	0.4×10^{-3}
NOV	58	0.13	5.18 ± 0.05	451 ± 4	1.0×10^{-3}

decrease of medium polarity; the lower solvation capacity of MeOH facilitates the formation of a polar excited state of the emissive twisted internal charge transfer state of LA.

Both the fluorescence increase and the rate of hydrolysis decrease observed in aqueous SDS solutions indicate the strong binding of LA to micelles. We assume a simple two-shell spherical model of SDS micelles at concentrations close to the cmc, with an inner hydrocarbon core and an outer concentric polar shell that contains the head groups ($-OSO_3^-$), a fraction β of the counterions (Na^+), and water (and perhaps the first methyl group of the hydrocarbon chain).[22,24]

A look at Fig. 2b and 3a indicates that the cationic form of the LA binds more strongly than the neutral form as a consequence of electrostatic interactions with the negatively charged micellar interface.

The polarity of the surface of SDS micelles depends on the micelle aggregation number, N_A, in such a manner that the hydration number per surfactant molecule decreases with N_A: the highest hydration is observed for the smallest N_A.[22] Under the conditions of the present experiments (low salt concentrations and low [SDS]) we can suppose small variations of N_A close to the value measured at the cmc (N_A = 50); in other words, within the interval of [SDS] analysed here, the polarity of the micellar interface does not change significantly. Nevertheless, it can be noted that values of fluorescence emission at saturation, I_F^m, depend on the nature of the LA molecule; for instance, in the case of PAM, values of 0.8 or 1.3 (much lower than those measured at high MeOH percentages) were observed with neutral or cationic forms, respectively (Fig. 2b and 3a), but the opposite was the case when the drug was TCA (Fig. 3b). High I_F^m values mean lower water content in the microenvironment sensed by the probe. One possible explanation would assume different binding modes of PAM and TCA, with insertion of either the primary (or secondary) amine or the tertiary amine end first. As the aniline moiety is uncharged under the experimental conditions of fluorescence measurements—a requisite to observe fluorescence—and the presence of the *n*-butyl-substituent in the TCA molecule, it is reasonable to assume this part of the TCA molecule enters first inside the micelle, with a degree of protrusion depending on the state of protonation of the tertiary amine group, $-N(CH_3)_2$, since the electrostatic attractions with the sulfate head groups of the SDS surfactant bring the positively charged TCA molecules out from the micellar interface. By contrast, in the case of NOV or PAM at least two different binding modes can be postulated, as a result of the balance in the interactions of the hydrophilic H_2N- group and the more hydrophobic $-N(CH_2CH_3)_2$ group (neutral) with the microenvironment: in alkaline medium, the tertiary amine group enters first, but the opposite could occur in neutral or acid medium, *i.e.*, under

conditions of a protonated tertiary amine group. The former configuration would explain the low I_F^m values measured in alkaline medium if the fluorophore moiety (the phenyl ring) remains in the outer polar shell of the micelles, and are also supported by the kinetic experiments. The ester function oriented to inside the micellar aggregates remains protected from the attack of the anionic nucleophile, OH^-, which is excluded from the micellar surface due to electrostatic repulsions. On the other hand, the analysis of the binding constants, K_s, obtained, for instance, in alkaline medium, shows that the highest value is obtained with TCA and the lowest one with PAM. Taking into account the amphiphilic character of these compounds, the results are consistent with the hydrophobic character of the probes: TCA could be approximated to a 14-C atoms chain length, whereas NOV, to a 10-C chain length, and in the case of PAM the presence of the amide bond increases both the flexibility and the polarity of the chain.

Conclusions

From these studies on fluorescence emission in water–methanol mixtures compared with those in aqueous solutions of sodium dodecyl sulfate, along with the results of electric conductance and of rates of alkaline hydrolysis of the ester function of LA in aqueous surfactant solutions, it can be concluded that the presence of these amphiphilic probes induces micellization. This fact can be understood as the presence of local anaesthetics alters interfacial properties, which are considered primary parameters that determine the anaesthetic effects, for which LA act through the closure of the sodium channels of nerve membranes. For the proper understanding of this blocking action, it is of interest to learn about the distribution of the anaesthetics throughout membranes, which systems are mimicked by micellar interfaces. The physicochemical characterization of the ternary water/SDS/LA systems near critical micelle concentration of SDS indicates self-aggregation giving rise to small premicellar aggregates that dramatically alter both the steady-state fluorescence emission and the reactivity of the drugs.

Acknowledgements

Financial support from the Dirección General de Investigación (Ministerio de Educación y Ciencia) of Spain and FEDER (Project CTQ2005-07428/BQU) and Xunta de Galicia (Project PGIDIT06PXIC103152PN) is gratefully acknowledged.

References

1 H. Y. Erbil, *Surface Chemistry of Solid and Liquid Interfaces*, Blackwell Publishing Ltd, Oxford, UK, 2006.
2 J. H. Fendler, *Membrane Mimetic Chemistry*, John Wiley & Sons, New York, 1982.
3 C. A. Bunton, F. Nome, F. H. Quina and L. S. Romsted, *Acc. Chem. Res.*, 1991, **24**, 357.
4 F. M. Menger and C. A. Littan, *J. Am. Chem. Soc.*, 1991, **113**, 1415.
5 F. M. Menger and J. S. Keiper, *Angew. Chem., Int. Ed.*, 2000, **39**, 1906.
6 R. Muzzalupo, M. R. Infante, L. Péres, A. Pinazo, E. F. Marques, M. L. Antonelli, C. Strinati and C. La Mesa, *Langmuir*, 2007, **23**, 5963.
7 T. Sakai, Y. Kaneko and L. Tsujii, *Langmuir*, 2006, **22**, 2039.
8 S. K. Ghosh, A. Pal, S. Kundu, M. Mandal, S. Nath and T. Pal, *Langmuir*, 2004, **20**, 5209.
9 S. Ghosh, A. Krishnan, P. K. Das and S. Ramakrishnan, *J. Am. Chem. Soc.*, 2003, **125**, 1602.
10 N. M. van Os, J. R. Haak and L. A. M. Rupert, *Physico-Chemical Properties of Selected Anionic, Cationic and Nonionic Surfactants*, Elsevier, Amsterdam, 1993.
11 P. T. Frangopol and D. Mihailescu, *Colloids Surf., B*, 2001, **22**(1), 3.
12 P. T. Frangopol and M. S. Ionescu, *Curr. Top. Biophys.*, 1993, **2**, 199.
13 H. Kamaya, J. J. Hayes, Jr and I. Ueda, *Anesth. Analg. (N. Y.)*, 1983, **62**, 1025.
14 A. Domínguez, A. Fernández, N. González, E. Iglesias and L. Montenegro, *J. Chem. Educ.*, 1997, **74**, 1227.
15 E. Iglesias, *Langmuir*, 1988, **14**, 5764.
16 D. D. Perrin, B. Dempsey and E. P. Serjeant, *pK_a Prediction for Organic Acids and Bases*, Chapman and Hall, London, 1981.
17 R. Stewart, *The Proton: Applications to Organic Chemistry*, Academic Press, Orlando, Florida, 1985, ch. 3.
18 E. Iglesias-Martínez, I. Brandariz and P. Penedo, *Chem. Res. Toxicol.*, 2006, **19**, 594.
19 (*a*) T. Förster, *Naturwissenschaften*, 1949, **36**, 186; (*b*) J. F. Ireland and P. A. H. Wyatt, in *Advances in Physical Organic Chemistry*, ed. V. Gold and D. Bethell, Academic Press, London, 1976, vol. 12, p. 132; (*c*) D. D. Perrin, B. Dempsey and E. P. Serjeant, *pK_a Prediction for Organic Acids and Bases*, Chapman and Hall, London, 1981, ch. 6.
20 W. Retting, *Angew. Chem., Int. Ed. Engl.*, 1983, **15**, 971.
21 K. Kalyanasundaram, in *Photochemistry in Organized & Constrained Media*, ed. V. Ramamurthy, VCH Publishers, UK, 1991, ch. 2.
22 B. I. Bales, L. Messina, A. Vidal, M. Peric and O. R. Nascimento, *J. Phys. Chem. B*, 1998, **101**, 10347.
23 E. Iglesias, *J. Org. Chem.*, 2006, **71**, 4183.
24 M. Almgren, F. Grieser and J. K. Thomas, *J. Am. Chem. Soc.*, 1979, **101**, 2021.

